IEEE Access
Multidisciplinary | Rapid Review | Open Access Journal

Received January 16, 2017, accepted February 7, 2017, date of publication February 22, 2017, date of current version March 15, 2017.

*Digital Object Identifier 10.1109/ACCESS.2017.2672818*

# Active Thermoelectric Cooling Solutions for Airspace Applications: the THERMICOOL Project

**EMMANUEL KARAMPASIS[1], NICK PAPANIKOLAOU[2], (Senior Member, IEEE), DIONISIS VOGLITSIS[2], MICHAEL LOUPIS[1], (Senior Member, IEEE), ANASTASIOS PSARRAS[2], ALEXANDROS BOUBARIS[2], DIMITRIS BAROS[2], AND GIORGOS DIMITRAKOPOULOS[2]**

[1]Innovative Technologies Centre S.A., 11633 Athens, Greece
[2]Electrical & Computer Engineering Department, Democritus University of Thrace, 67100 Xanthi, Greece

Corresponding author: N. Papanikolaou (npapanik@ee.duth.gr)

This work was supported by the European Union's Seventh Framework Programme (FP7/2007-2013) for the Clean Sky Joint Technology Initiative under Grant 632436.

**ABSTRACT** To increase the reliability of aerospace electronics and reduce their overall power consumption, we investigated the possibility of incorporating active thermoelectric cooling (TEC) solutions. The harsh avionic environment demands sophisticated active control schemes that enable the achievement of high coefficient of performance. The positive effect of active PWM control has been validated both in simulation and on a working laboratory prototype that allowed us to clarify the pros and cons of the incorporation of TEC techniques in avionics applications. This paper has been performed under the framework of CLEAN SKY—THERMICOOL project.

**INDEX TERMS** Aerospace electronics, pulse width modula-tion, thermoelectric devices.

## I. INTRODUCTION

Sustainable energy management has become an issue of grave and global concern over the last two decades; the exploitation of renewable energy sources and the adaptation of energy efficiency measures and practices, by incorporating smart energy management algorithms, are key technologies for the reduction of fossil fuels share worldwide. To this direction, the complete electrification of aircrafts is of major importance; viable technologies for this purpose include devices and systems that take advantage of thermoelectricity. The thermoelectric (TE) effect includes the transformation of heat to electric energy and vice versa and its applications can consequently traverse two domains: (a) Electricity generation from heat sources such as power plants, factories and motor vehicles, by exploiting the Seebeck effect; (b) cooling (or heating) using solid-state thermoelectric devices that can exploit the Peltier effect [1]–[4]. The exploitation of this energy-conversion phenomenon allows the design of reliable systems, built with solid-state devices that enable long-life operation, do not need any moving parts and leave any toxic residuals, thus contributing to the goal of low environmental footprint.

Thermoelectric coolers have been successfully used in commercial cooling applications with high heat dissipation requirements. In electronic applications, a well-designed thermoelectric cooler forces heat to flow from the cold surface to the hot one, maintaining the junction temperature of a device below a safe temperature, by pumping heat away from the device. In order to improve their performance, active thermoelectric cooling solutions have also been proposed, based on active PWM control of the supplying current [5]. To this direction, in the framework of CLEAN SKY – THERMICOOL project, the study and development of an innovative thermoelectric cooling (TEC) solution for avionic application with maturity level TRL5, low power consumption and high efficiency has been performed. The study focused on the incorporation of an active TEC solution to achieve high coefficient of performance (*COP*) values. In addition, the construction of a laboratory test bench took place, for the conduction of tests.

THERMICOOL is the acronym of the project entitled "Thermoelectric cooling using innovative multistage active control modules (Project number: 632436)" and it consists of three main technical Work Packages (WPs); WP1 was entitled "Bibliographical Review" and included the bibliographical review of thermoelectric materials and cooling solutions, as well as a survey on the available commercial systems. The main theoretical analysis of the project was implemented in WP2, which was entitled "Technology Selection"; in more details, an extended finite element (FEM)

modeling and simulation analysis has been carried out for the specific case study provided by the Topic Manager (Labinal Power Systems) and the final technology selection has been decided, based on the FEM analysis results. Finally, in WP3 entitled "Experimental Validation" the construction of the laboratory test bench took place, as well as the conduction of an extended series of evaluation tests.

In the following Sections the tasks performed in these WPs will be analytically presented and the major project findings will be discussed.

## II. BIBLIOGRAPHICAL REVIEW

### A. PROJECT CHALLENGES AND APPROPRIATE TE MATERIALS

Some of the challenges faced in THERMICOOL project are the following:

- Selecting the right TE materials which would balance cost against efficiency. Materials with an increased figure of merit ($ZT \gg 1$) are needed to get more cooling power. However, building them can be hard and costly, since complex fabrication processes might be involved.
- Matching the temperature of the heat source to the proper thermoelectric module type. Part of the problem is that the source temperature varies under normal operation. The temperature of the engine can vary from $-55°$C to $+125°$C, while the ambient temperature from $-70°$C to $+160°$C. Therefore, the temperature gradient between the hot and the cold side of the device can get as high as 200°C. Apart from selecting the right materials, which could perform efficiently within the target temperature ranges, care should be taken to avoid damaging the module at peak temperatures.
- Maintaining a satisfactory power conversion for the cooling system as a whole. Although a high-$ZT$ material is a prerequisite for an efficient device, it cannot guarantee an efficient performance in total. In this project, a high coefficient of performance ($COP > 1$) was also required, in order to provide a cooling power of 100W with a power density of 30 W/cm$^2$.

Although TE materials have been available since the late 1950's, their low efficiency ($ZT < 1$) prevented their widespread applications [6], [7]. Breaking the $ZT = 1$ barrier was made possible in the 1990's, through two different research approaches: one of exploring new materials, with complex crystalline structures, and the other of reducing the dimensions of the materials [8]. Currently available materials include: $Bi_2Te_3$-based and SiGe alloys, skutterudites (e.g. $CoSb_3$, $CoP_3$, $CoAs_3$, $RhSb_3$, $IrSb_3$ etc.), clathrates (e.g. $(Ba,Sr)_8(Al,Ga)_{16}(Si,Ge,Sn)_{30}$), half-heuslers (e.g. $Zr_{0.5}Hf_{0.5}CoSb_{0.8}Sn_{0.2}$), oxides, and lead antimony silver tellurium based materials, such as $AgPb_mSbTe_{2+m}$ (LAST), $Ag(Pb_{1-x}Sn_x)_mSbTe_{2+m}$ (LASTT), $Na_{1-x}Pb_mSb_yTe_{m+2}$ (SALT) and $NaPb_{18-x}Sn_xSbTe_{20}$ (SALTT) [6]–[35].

Despite the wide variety of available materials, not all of them are suitable for any application. Therefore, selecting the appropriate material is determined by the type of application and the expected operating temperatures. For instance, a material with a maximum $ZT = 1.5$ at temperature of 800K, would be useless in a cooling system of a microcontroller operating close to room temperatures. With this in mind, only materials efficient in the device ambient and target operating temperatures (approximately 200K to 400K) were considered. For refrigeration applications in around room temperatures, bismuth telluride alloys have been proven to possess the highest figure of merit for both p- and n-type thermoelectric systems [35]. Materials that meet those requirements of THERMICOOL project are shown in Table 1, along with their maximum $ZT$ values and the corresponding operation temperatures. Their figure of merit as a function of temperature is illustrated in Fig. 1 (values are those reported by the corresponding publications).

**TABLE 1. Selected TE materials.**

| Material | ZT | T(°K) | Ref |
|---|---|---|---|
| $Bi_{0.52}Sb_{1.48}Te_3$ | 1.4 | 370 | [6] |
| $Cu_{0.01}Bi_2Te_{2.7}Se_{0.3}$ | 1.1 | 300 | [9] |
| $Bi_{0.45}Sb_{1.55}Te_3$ | 1.75 | 270 | [7] |
| $CsBi_4Te_6$ | 0.8 | 225 | [29] |
| $Tl_9BiTe_6$ | 1.2 | 500 | [30] |
| $(Bi_{0.25}Sb_{0.75})_2Te_3$ | 1.4 | 310 | [31] |
| $AgPb_{18}SbTe_{20}$ | 2.1 | 800 | [23] |
| $Bi_{0.52}Sb_{1.48}Te_3$ | 1.56 | 300 | [8] |

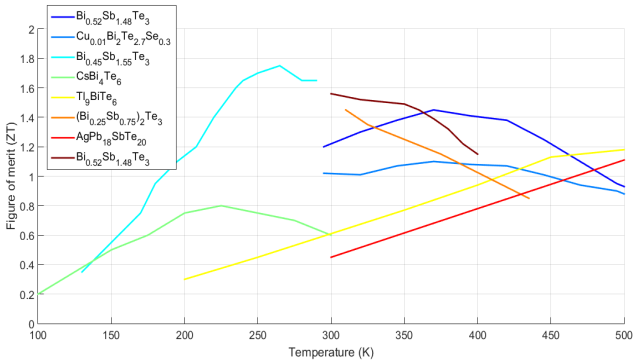


**FIGURE 1. Figure of merit for selected materials. Data are collected by the relevant literature in Table I and plotted using linear interpolation.**

### B. CASE STUDIES

Although the figure of merit is a crucial factor for determining a material's efficiency, we base our selection on the COP factor that depicts the efficiency of the thermoelectric system as a whole. For a cooling TE system that operates in an ambient temperature of $T_h$, with a device temperature of $T_c$, and a material of figure of merit $ZT$, its optimum coefficient of performance is given by [2]:

$$COP_{opt} = \frac{\gamma T_c - T_h}{(T_h - T_c)(1+\gamma)} \quad (1)$$

$$\gamma = \sqrt{1+ZT} \quad (2)$$

In order to determine the efficiency of the selected materials, various case studies on the selected materials are

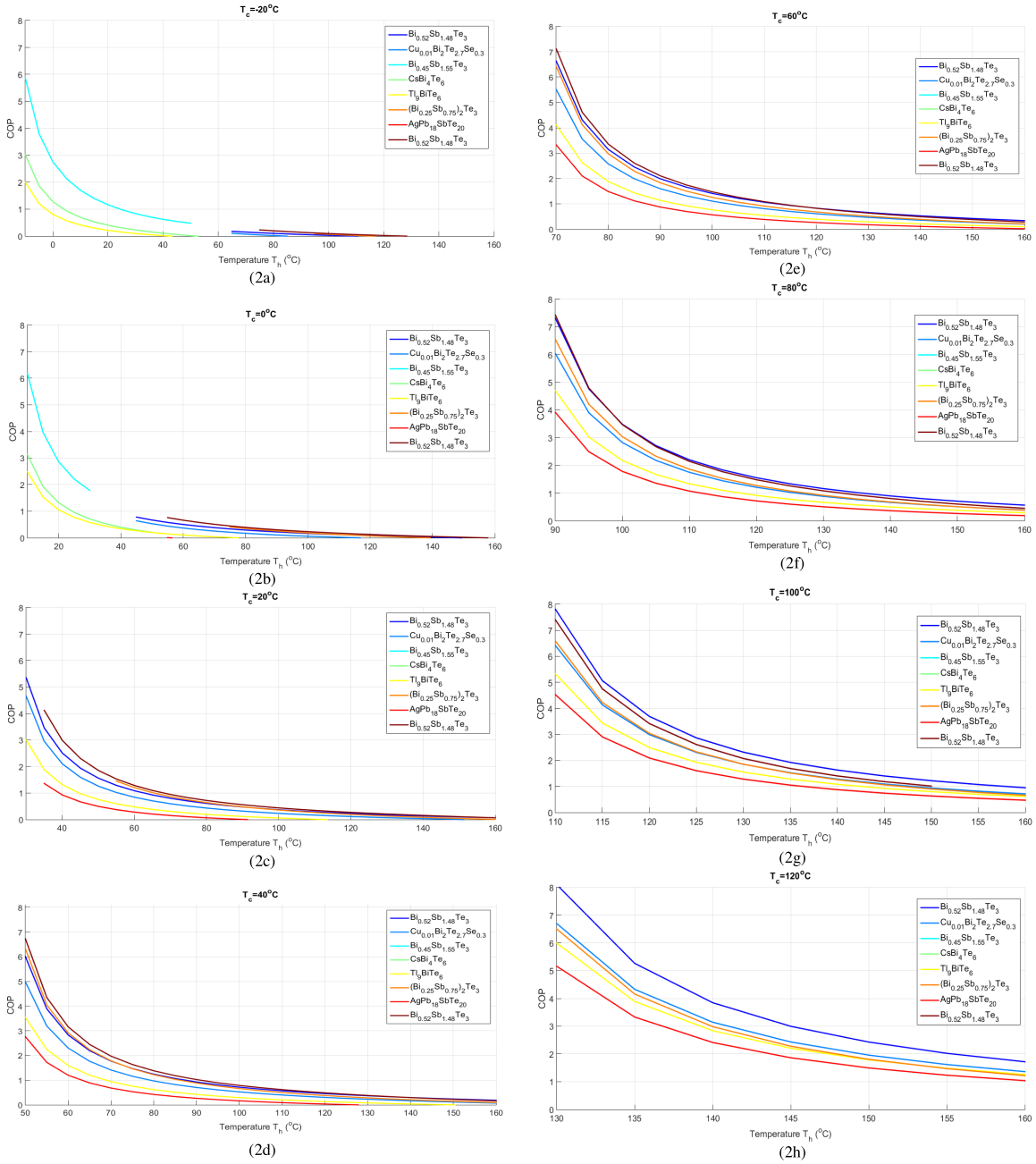


**FIGURE 2.** ***COP*** **as a function of $T_h$, $T_c$, for the selected case studies.**

presented in Figs 2a-2h, assuming different values of $T_h$ and $T_c$. Calculation of the $ZT_m$ value is made through spline interpolation of the known points for each material, for the mean temperature $T_m = (T_c + T_h)/2$. Values of $T_m$ that are out of the range of values reported by the corresponding reference are omitted, resulting to interrupted *COP* plots. For each case study, a constant $T_c$ is assumed, and *COP* is plotted for $T_h$ values that vary from $T_c + 10°\text{C}$ to a maximum of 160°C.

According to the derived *COP* trends, a *COP* factor above unity can be obtained at certain temperature ranges, for every material. In fact, for small ambient-to-device temperature differences, around 10-20°C, *COP* can theoretically reach extreme values, even greater than 2.0. However, efficiency degrades significantly as the temperature difference is further increased. Regardless of the device temperature, there is always a hot ambient temperature, over which, selecting a high-*ZT* material makes negligible difference. Also, the system's behavior in very low temperatures (<0°C) is of concern, since the number of efficient available materials is limited in that range.

Therefore, according to the target specifications, especially concerning operating temperatures, guaranteeing a constant satisfactory behavior in terms of performance (*COP*>1), is not a straightforward task. The final material selection

depends on the expected temperature fluctuations: e.g. is it possible that ambient temperatures may frequently reach the extreme values; if this is the case, a versatile system would be required that involves an array of TE coolers, built from different materials. Each one of them would own different characteristics, i.e. different temperature that maximizes *ZT*, and a proper controller would turn on the appropriate device, according to the ambient temperatures. The examined case studies highlight that high *COP* values can be met by BiSbTe alloy materials while still allowing them to operate in a harsh avionics environmental conditions Nevertheless, the selection of an appropriate material is not enough and active PWM control techniques are needed for maintaining high *COP* values under the worst case operating and environmental conditions.

## III. TECHNOLOGY SELECTION

### A. SYSTEM SPECIFICATIONS

Typical avionic equipment is mainly composed by a power core (power modules, sensors etc) and electronic boards (monitoring, control, supply board). The thermal management of this equipment is done by internal conduction and external air convection.

For such equipment, electronic boards are populated with maximum junction temperature rating of 125°C. However, the qualifications for next equipment generation will require higher functional capacity, implying higher heat dissipation. New thermal solutions are highly required to allow this evolution, by creating local cold point or/and open new thermal paths. Thermoelectric cooling technology is targeted to restore a high thermal margin for an electronic control module, of mezzanine type, mounted on a support board in this kind of equipment.

The baseline configuration defined by the project requirements should follow the following setup:

- Overall size of the equipment: 500mm × 120mm × 300mm
- Total steady state permanent mean equipment heat dissipation: 26W
- Ambient temperature range: [−55°C; 95°C]
- Heat exchange coefficient between equipment chassis and external air: 10W/m$^2$/K
- Mezzanine board dimensions: 85mm × 93mm
- Distance from mezzanine to equipment cover: 25mm (the mezzanine board is parallel to the cover of the equipment with dimensions 500mm × 300mm)
- Mezzanine board could be considered as thermally separated from its support board
- Mezzanine board heat rejection is localized in the PCB, centered and distributed on 3/4 of the mezzanine area

Fig. 3 depicts the block diagram of the system under study. It consists of a power core which is thermally isolated by the mezzanine board; the mezzanine board with the above mentioned specifications, which is the component that has to be actively cooled; and the support board which is a PCB with several heat sources placed on its surface. The specifications for the active TEC solution are the following:

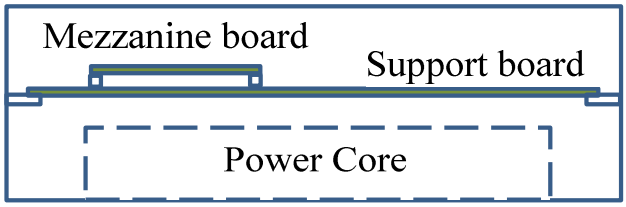


**FIGURE 3.** Schematic view of equipment / Cooling of an electronic control module for power electronic equipment mounting on engine fan case.

- R1 Thermoelectric cooler shall permanently reject at least 7W from the mezzanine board to external air.
- R2 Thermoelectric cooler total heat rejection shall not increase mean temperature equipment of more than 5°C (heat rejection is composed of mezzanine board heat dissipation plus TEC supply).
- R3 Mezzanine board mean temperature shall not exceed 95°C whatever the external ambient temperature from −55°C to +95°C.
- R4 Mezzanine board mean temperature shall not be less than −40°C, whatever the external ambient temperature in the range −55°C to +95°C.

### B. SELECTION OF OPTIMUM TEC TECHNOLOGY - SYSTEM MODELING

According to the analysis in Section II, and for hot side temperatures between 300K and 450K, the use of BiSbTe alloy is the most appropriate solution. In more details, Fig. 1 shows clearly that the *ZT* for this type of material is well above 1.2 for the above mentioned temperature range. Hence, in the present thermal analysis the use of $Bi_{0.52}Sb_{1.48}Te_3$ TEC technology is being considered, leading to a *COP* factor greater than 1.0 for cold side temperatures between 90°C - 95°C and hot side temperatures up to 160°C.

The TEC simulation model (for this thermal analysis) is based on the existing TEC general model of "*FloTHERM XT*". The electrical – thermal parameters' set corresponds to the data, which have been provided for $Bi_{0.52}Sb_{1.48}Te_3$ TEC technology in Section I. Additionally, the TEC module dimensions are selected to be similar with the ones of commercial modules operating under the same temperature range.

The modeling of the system has been made by taking into account the electrical and geometrical specifications, as described in the previous Subection. According to these requirements, the electronic equipment is mainly composed by a power core and electronic boards (monitoring, control, supply board). To this end, the overall system model includes the PCB, which is modeled as a Uniform Heat Source (Copper Layer) and an FR4 bottom layer (Support Board), the Mezzanine, the Power Generator (PG) placed on the top of the Mezzanine, ,the Heat Transfer element and the Insulator, all enclosed in an aluminum box chassis (Enclosure). The Power Core shown in Fig. 3 is omitted from the simulation model because it is supposed to be thermally insulated from the rest

**TABLE 2. Geometrical and material specifications of the utilized components.**

| COMPONENT | DIMENSION (mm) | MATERIAL | POWER (W) |
|---|---|---|---|
| Thermoelectric Cooler | 40 x 40 x 4.1 | Ceramic | 103.1 / 150 / 200 |
| PG | 77 x 77 x 2 | Ceramic | 7 |
| Mezzanine | 85 x 93 x 2 | FR4 | - |
| Heat Transfer | 77 x 77 x 11 | Aluminum 5052 | - |
| Copper Layer | 496 x 296 x 0.035 | Copper | 20 |
| Support Board | 496 x 296 x 2 | FR4 | - |
| Mechanical Stiffener | 8 mm thickness, roundup | Aluminum 5052 | - |
| Insulator | 496 x 296 x 6 | Ideal Insulation | - |
| Enclosure | 500 x 300 x 47 | Aluminum 5052 | - |
| Gap Filler | 0.035 mm thickness | Gap Filler | - |

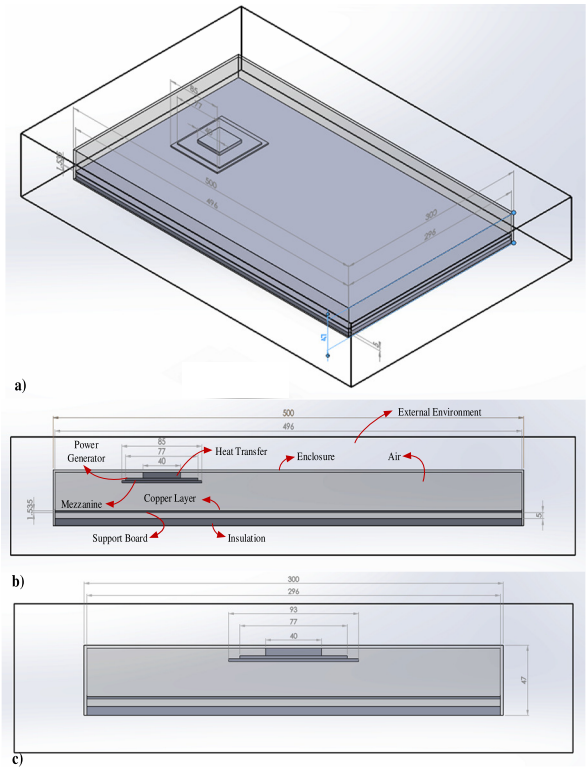


**FIGURE 4. Simulated Test bench: a) perspective view, b) left side view, c) front side view.**

of the system. The geometric and electrical characteristics of the utilized models are summarized in Table 2, while their relevant location in the framework and their physical representation are depicted in Fig. 4. It must be noted that the TEC element is initially absent from the analysis and from the system representation in Fig. 4. The introduction of the TEC module is presented in Fig. 5, located between the mezzanine board and the Heat Transfer element.

To fit the Mezzanine board and the power generator exactly at the bottom side of the Enclosure we lifted the mezzanine board; a thick aluminum plate was used as the thermal transfer means between the mezzanine and the Enclosure.

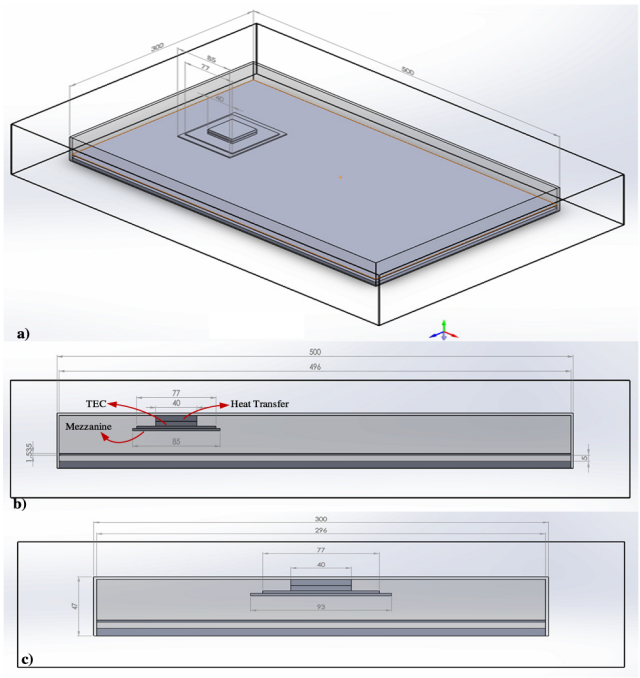


**FIGURE 5. Simulated Test bench including the TEC element: a) perspective view, b) left side view, c) front side view.**

This contributes to the generation of an interface between the Power Generator and the Enclosure, which allows the conduction of heat transfer to the Enclosure and subsequently, the heat rejection from the Enclosure to the environment, due to both convection and radiation mechanisms.

## IV. THERMAL SIMULATION RESULTS

This section focuses on the presentation of the thermal simulation results of the above described system. Five thermal flow scenarios (Sub-cases I-V) have been considered, which are listed below:

i) Model with TEC ($Q_{max} = 103.1W$) at +95°C, 2A operational current
ii) Model with TEC ($Q_{max} = 150W$) at +95°C, 2A operational current
iii) Model with TEC ($Q_{max} = 200W$) at +95°C, 2A operational current
iii.1) Updated Model with TEC ($Q_{max} = 200W$) at +95°C, 2A operational current
iv) iii.2) Updated Model with TEC ($Q_{max} = 200W$) and Gap Filler at +95°C, 2A operational current Model with TEC ($Q_{max} = 200\ W$) at −55°C, 2A operational current
v) Model with TEC ($Q_{max} = 200\ W$) at −55°C, 1A operational current

The results considering the Mezzanine Board are presented in Table 3, where the above mentioned flow thermal scenarios have been considered and TEC elements with various $Q_{max}$ have been tested and evaluated. According to the conducted thermal analysis and the corresponding results, it is concluded that the mezzanine board has to be lifted in order to

**TABLE 3. FlowTherm simulation results.**

| Sub-case | Description | Requirements R1 | R2 | R3 | R4 |
|---|---|---|---|---|---|
| i) | Model with TEC ($Q_{max} = 103.1\ W$) at +95°C, 2A operational current | √ | X | X | √ |
| ii) | Model with TEC ($Q_{max} = 150\ W$) at +95°C, 2A operational current | √ | X | X | √ |
| iii) | Model with TEC ($Q_{max} = 200\ W$) at +95°C, 2A operational current | √ | √ | √ | √ |
| iii.1) | Updated Model with TEC ($Q_{max} = 200\ W$) at +95°C, 2A operational current | √ | √ | √ | √ |
| iii.2) | Updated Model with TEC and Gap Filler ($Q_{max} = 200\ W$) at +95°C, 2A operational current | √ | √ | √ | √ |
| iv) | Model with TEC ($Q_{max} = 200\ W$) at –55°C, 2A operational current | √ | X | √ | √ |
| v) | Model with TEC ($Q_{max} = 200\ W$) at –55°C, 1A operational current | √ | √ | √ | √ |

reduce the TEC thermal resistance with the enclosure, thus transferring the heat to the environment more effectively. Furthermore, it has been shown that natural cooling is adequate for ambient temperatures less than 63°C.

In case of ambient temperatures greater than 63°C, a TEC element is required in order for the mezzanine temperature to meet the set limitations. Regarding the selection of the TEC element, it has been shown that TECs with $Q_{max} < 200\ W$ are inadequate to cool sufficiently the mezzanine board, while TECs with $Q_{max} \cong 200\ W$ of $Bi_{0.52}Sb_{1.48}Te_3$ TEC technology, are able to cool the mezzanine safely below the maximum permissible temperatures. It is noted that a closed loop is necessary in order to regulate the TEC current and to achieve safe operating temperatures. Finally, it has been shown that the bottom temperature limitations are well respected, as the mezzanine temperature is well above the minimum temperature limit of −40°C by 17.5°C.

## V. EXPERIMENTAL EVALUATION

### A. EXPERIMENTAL SETUP

The overall experimental setup is shown in Fig. 6; it consists of the Thermal Closet, the Air Heating System (blower, heaters, and temperature controller), the Power Supplies (for the supply of the heat sources inside the enclosure), the Heat Flux and Temperature Measurements and the Line Panel (for the system overall operation management and protection). In addition, the DSPACE platform and the laboratory constructed PWM converters are included in the experimental setup for the implementation of the active PWM control schemes.

Figs 7 and 8 illustrate the laboratory construction of the enclosure and the components inside it. For better

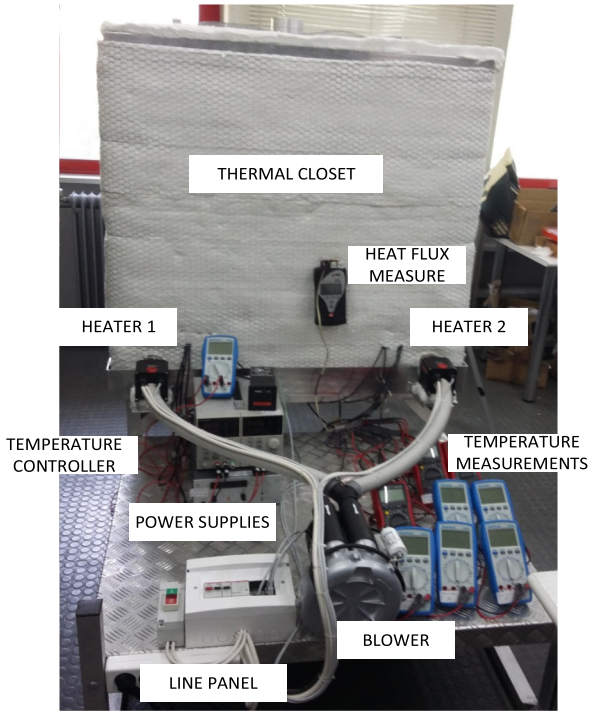


**FIGURE 6. Illustration of the experimental setup.**

**FIGURE 7. Laboratory enclosure (top side).**

understanding the laboratory construction, Fig. 9 illustrates the schematic of the PCB layer. The enclosure is an aluminum box chassis; two thermistors (T3, T4) are placed on the top (outer) side of the enclosure. Regarding the mezzanine, it has been emulated as a copper layer (0.1 mm thickness) in thermal contact with an aluminum plate (2 mm thickness) from down to top. To incorporate the 7W Power Generator, a resistor bank in thermal contact with the copper layer has been used. It has to be mentioned that a pair of Heat Flux Sensors has been placed on the hot and cold sides of TEC1, in order for the heat flow to be measured; heat flux data were transferred to a dedicated Data Logger. A thermal paste has been used to improve the thermal conduction of all components that have to be in thermal contact with the mezzanine. Finally, two thermistors (T9, T10) have been placed on the

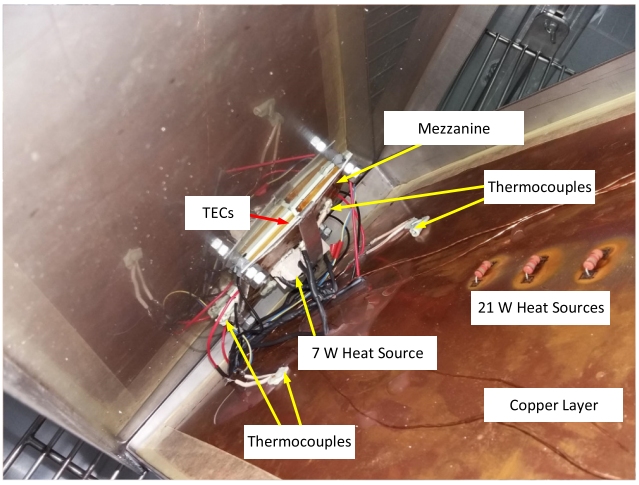


**FIGURE 8.** Illustration of the components inside the enclosure.

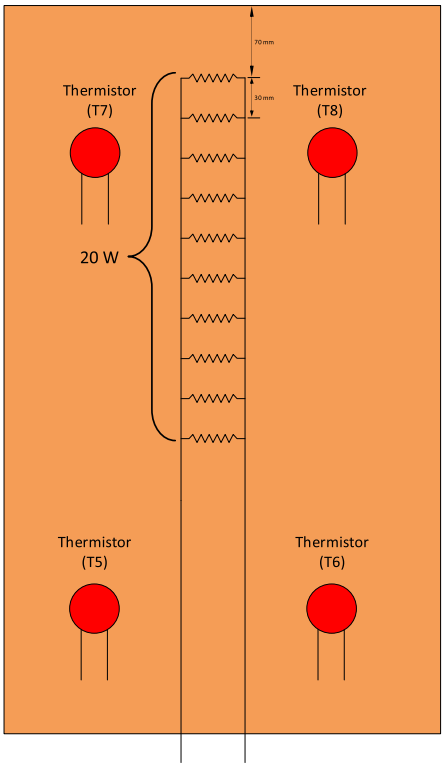


**FIGURE 9.** Schematic of the PCB (copper layer).

bottom (aluminum) layer of the mezzanine board for temperature measurements. Regarding the PCB, the heat source of 21W consists of ten Resistors connected in parallel, as depicted in Fig. 9; hence it is not possible to be uniformly distributed throughout the copper layer (as it had been considered in the simulation process), leading – inevitably – to temperature divergences between the real experiment and the simulation results. Nevertheless, this approach does not cancel the experimental results. Moreover, four thermistors (T5, T6, T7, and T8) have been placed on the top side of the copper layer (as shown in Fig. 9) in order the temperature to be measured. It is noted that all necessary signal and power

**TABLE 4.** List of components for the laboratory setup.

| A/A | Component | Description |
|---|---|---|
| 1 | ND03U00105K (AVX) | Thermistors, 150°C |
| 2 | Sequoia SHF Series | Heat Flux Sensors, 40X40mm, 12.6μV/(W/m$^2$) |
| 3 | Resistors | Various Types |
| 4 | M1220 (SENSOMETRIx) | Data Logger |
| 5 | Loird Thermal Paste | Thermal Paste (0.1K/W) |
| 6 | PCB (copper layer) | 35μm Copper Layer |
| 7 | Delta Electronik | Switch Mode Power Supplies |

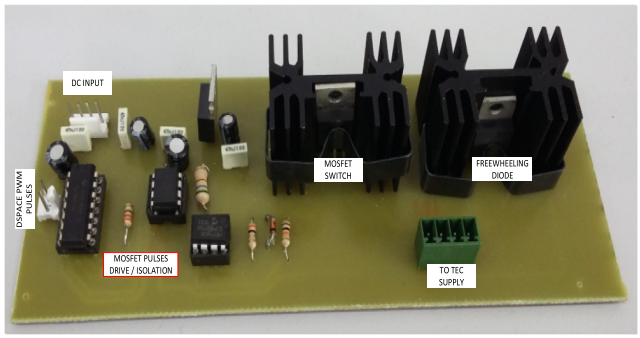


**FIGURE 10.** Experimental prototype of the dc/dc step down (buck) converter.

cabling has been constructed, by means of multicore copper wires with a maximum operating temperature of +200°C. Table 4 summarizes the components used for these constructions and measurements.

### B. ACTIVE PWM CONTROL

Active PWM control of the TEC modules has been implemented by means of a buck dc/dc converter prototype, depicted in Fig. 10. Note that the converter generates current pulses at its output stage, i.e. there is not any output filter capacitor. The control scheme, which is developed by means of MicroLabBox, provided by dSPACE, is based on the well-known PWM technique. The aim of the control is to generate pulses that drive the converter power switch accordingly, so that the TEC module is supplied by current pulses of an appropriate pattern. To this end, two different switching patterns, based on the PWM, have been developed; the classical Single PWM Carrier (SPC), and the proposed Double PWM Carrier (DPC).

The principle of the SPC pattern is the basic PWM one, illustrated in Fig. 11; the produced pulses are generated by the comparison of two signals. That is a high frequency signal denoted as $V_{carrier}$ and a dc-signal denoted as $V_{control}$. Applying these pulses to the buck converter of Fig. 10 the power switch (power MOSFET) duty cycle, $D_f$, defines the output converter voltage and current. The control scheme of SPC pattern is also summarized in Fig. 11.

The DPC pattern is produced by mixing a low frequency pulsing signal with the SPC output pulses as it can be seen

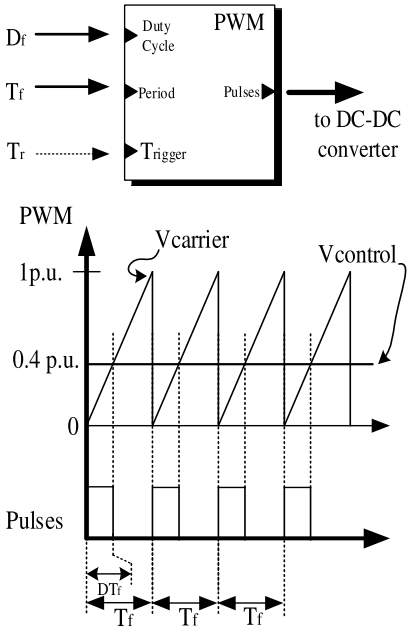


**FIGURE 11.** SPC pattern representation.

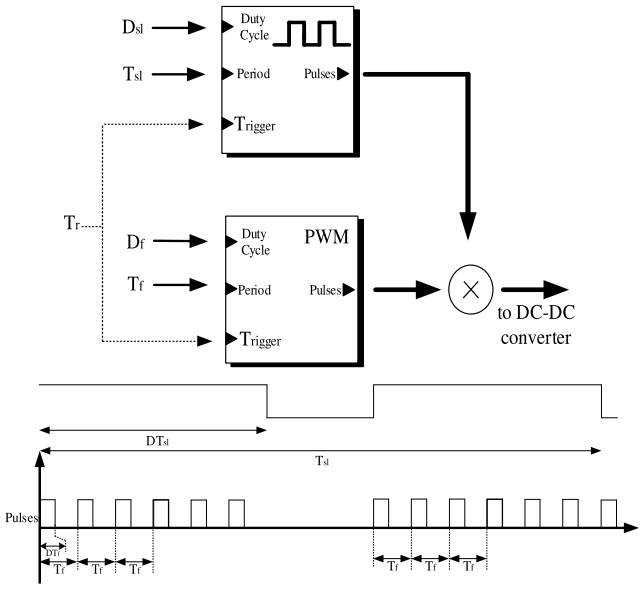


**FIGURE 12.** DPC pattern representation.

in Fig. 12. The duty cycle and period of this low frequency signal is denoted as $D_{sl}$ and $T_{sl}$ respectively. The output pulses generated by DPC resemble the pulses depicted also in Fig. 12.

### C. EXPERIMENTAL RESULTS

This paragraph is dedicated to the experimental results of the thermoelectric cooling application under harsh aeronautical conditions; having the MCPF-127-14-11-E as the basic single stage TEC Module, the experimental procedure considered the TEC configurations that are summarized in Table 5. Those experimental cases have been analytically tested in the experimental installation, against the requirements of the

**TABLE 5.** List of experimental cases under study.

| Experimental Case | TEC configuration | Control Method |
|---|---|---|
| CASE 1 | No TEC connection | Inactive |
| CASE 2 | 4 x MCPF-127-14-11-E electrically connected in series (single stage) | Constant current |
| CASE 3.1 | 4 x MCPF-127-14-11-E electrically connected in series (single stage) | Classical active PWM control (SPC) |
| CASE 3.2 | 4 x MCPF-127-14-11-E electrically connected in parallel (single stage) | Constant current |
| CASE 4 | 4 x MCPF-127-14-11-E electrically connected in parallel (single stage) | Classical active PWM control (SPC) |
| CASE 5 | 4 x MCPF-127-14-11-E electrically connected in parallel (single stage) | Novel active PWM control (DPC) |

**TABLE 6.** Experimental evaluation summary.

| Experimental Case | Critical ambient temperature that meets the project requirements | Remarks |
|---|---|---|
| CASE 1 | 63°C – 65°C | Results similar to the simulation outcomes |
| CASE 2 | 78°C | Restricted cooling capabilities |
| CASE 3.1 | 83°C | Improved cooling capabilities – small *COP* values |
| CASE 3.2 | 78°C | Restricted cooling capabilities |
| CASE 4 | 83°C – 85°C | Improved cooling capabilities – small *COP* values |
| CASE 5 | 95 °C – 97°C | Meets the project requirements |

THERMICOOL project, highlighting their Pros and Cons. The summary of the experimental procedure is summarized in Table 6.

In more details, Case 1 was initially tested at +63°C environmental temperature; this test was used as a reference one, in order to evaluate the effect of the considered thermoelectric cooling schemes, as well as to assess the validity of the system simulation model. The obtained results lead to the conclusion that the simulation studies are confirmed, regarding the critical condition for the mezzanine board average temperature to reach +95°C. It is noted that the difference between the experimental and the simulated average temperature values on the mezzanine surface was 2.6%. However, the difference between the minimum and maximum temperature values on the mezzanine surface, was quite smaller in the experiment than in the simulation results; this can be justified by the

fact that the thermal sources in the experimental setup were not uniformly distributed throughout the mezzanine and the copper layer (PCB) surfaces (as in the simulated model). For the same reason, there were also notable differences between the experimental and the simulation results concerning the maximum and minimum temperature values on the copper layer surface. Nevertheless, the average temperature value on the copper layer surface was close enough to the simulation results, having a small divergence of 5.9%. Finally, higher differences between the measured and the simulated temperature values on the enclosure surface existed; the fact that the measured temperatures were much smaller than the simulated ones can be justified by the air velocity due to the blower operation. Nevertheless, this part of the experimental setup is of lower importance. In summary, the temperature measurements at +63°C environmental temperature highlight the fact, that this is the critical condition for the average temperature value at the mezzanine surface. It is also deduced, that in the experimental setup the average temperature values at the mezzanine and the copper layer surface are in line with the corresponding simulated values, although small divergences exist between maximum and minimum temperature values.

Next, Case 1 has been tested at +95°C environmental temperature, which is the worst case scenario for the environmental temperature conditions. According to the obtained results we may conclude that the difference between the experimental and the simulated average temperature values at the mezzanine surface was 3.3%, while the difference between minimum and maximum temperature values at the mezzanine surface was quite smaller than in the case where the environmental temperature was +63°C; this can be justified by the fact that at such high temperatures the mezzanine surface was heated in a more uniformly way. On the other hand, the difference between the experimental and the simulated average temperature values was increased for the copper layer surface, reaching 11.4%. It is noted however, that the difference at the minimum temperature value has been drastically decreased, being only 3.1%. Once again, these results for the copper layer surface can be justified by the fact that the thermal sources in the experimental setup were not uniformly distributed throughout the mezzanine and the copper layer surfaces (as in the simulated model). Finally, the differences between the measured and the simulated temperature values on the enclosure surface have been also decreased drastically, below 3%; it has to be noted that the average temperature value on the enclosure surface is higher than in the simulation results, leading to the conclusion that the enclose thermal resistance was considerably higher than the one in the simulation process (taking also into account the positive presence of the air velocity due to the blower operation). This can be justified by the differences in the material used (AlMgSi-0.5 F22 aluminum alloy) as well as its higher thickness (in order to ensure the static safety of the thermal closet). As it will be shown onwards, the higher thermal resistance affects also the operation of TECs – leading to higher temperature differences between the cold and the hot sides ($\Delta T$). In summary, the temperature measurements at +95°C environmental temperature highlighted also the fact, that in the experimental setup the temperature values at the mezzanine surface are in line with the corresponding simulated values. On the other hand, higher divergence was observed for the average temperature value on the copper layer (PCB) surface, as a result of the heat sources distribution. Finally, the enclosure temperature values were now in line with the corresponding simulated values (although its thermal resistance was higher than in the simulation process).

Hence, the experimental results without any TEC operation have shown that the experimental setup was valid for the study of TECs' operational characteristics, despite the fact that there were some divergences between the experimental and the simulated temperature values.

After the experiments without utilizing any TEC module, the first thermoelectric cooling experiment took place, namely Case 2, considering the series connection of TECs. The electric power supply was regulated by means of a control loop that minimized the average TEC temperature value; for this purpose, the use of the Maximum Power Point Tracking (MPPT) control loop that was developed in the context of CLEAN SKY – RENERGISE project [36], has been modified and incorporated into the experimental process. It is noted that the MPPT controller time constant (averaging period) was set to 1sec, in order to account for the thermal inertia of the system. According to the obtained results, we may conclude that the series TEC connection was not suitable for the specific application. This was due to the fact that the total series resistance was very high (4 × 1.58 Ohm) and so the Joule effect restricted drastically the supplying current range, that leads to $COP$ values greater than 1.0. Consequently, the provided cooling power, $P_c$, was limited below 4W and consequently the TEC system managed to keep the average temperature value of the mezzanine surface below +95°C up to 78°C – 80°C ambient temperature values.

Next, Case 3.1 was evaluated, where the series TEC connection was subject to classical active PWM control (SPC pattern). Various tests were performed in order to identify the most suitable switching frequency; however, it seemed that frequency values between 500Hz and 1kHz had similar results, while higher frequencies increased notably the electric power consumption. This was due to the high series resistance and the skin effect that becomes dominant as frequency rises. It is noted that all measurements in this Case stand for steady state conditions (i.e. the MPPT controller is in steady state). Moreover, the temperature control loop was also active, by regulating the duty cycle value $D_f$. According to the obtained results, we may conclude that the use of the SPC pattern in series TEC connection improves its cooling capability; ,the critical temperature becomes as high as 83°C due to the higher $COP$ values at higher ambient temperatures. This is due to the lower electric power consumption, $P_{el}$, thanks to the switching supplied current. It is noted that even at +95°C ambient temperature, the classical active PWM method improved the temperature conditions on the

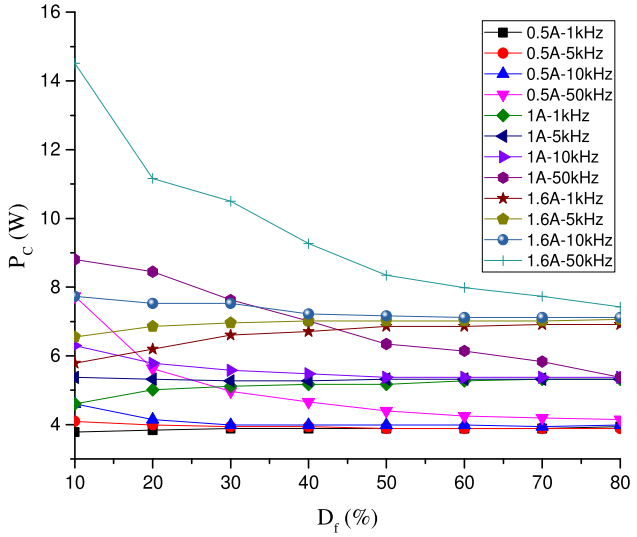


**FIGURE 13.** $P_c$ as a function of $D_f$, with $I$, $f_s$ being parameters (Parallel TEC connection).

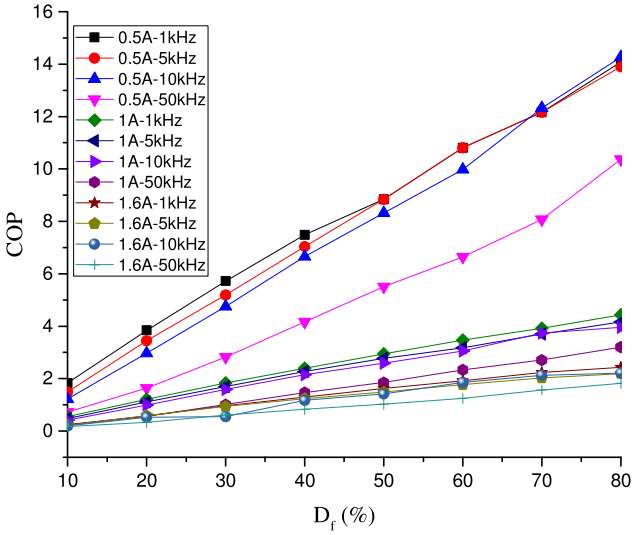


**FIGURE 14.** *COP* as a function of $D_f$, with $I$, $f_s$ being parameters (Parallel TEC connection).

mezzanine surface; notably, its ambient temperature value was reduced by 12.5°C. Nevertheless, the experiments so far have highlighted that the series TEC connection was not able to meet the project requirements and so the parallel connection had to be employed.

After the experiments considering the series connection, the parallel connection of TEC modules was established, initially driven by constant current, i.e. Case 3.2; as it was expected, constant current supply had similar results with the ones presented for the series TEC connection, supplied also by a constant current, i.e. the cooling power capability was reduced very quickly due to the rise of $\Delta T$.

Case 4 was a much more interesting case than the previous one, due to the classical SPC pattern that incorporated. Because of the parallel TEC connection, the Joule effect was less dominant, due to the drastically reduced equivalent resistance (1.58 / 4 Ohm) and so a wider switching frequency range could be exploited. In order to study the cooling behavior of the parallel connected system, a test was carried out; during this test, $P_c$ ad *COP* values were measured with the switching frequency, $f_s$, $D_f$, as well as the total average supplying current, $I$, being variable parameters. The test was performed at 83°C average temperature value on the mezzanine surface. The results of this test are depicted in Figs 13 and 14, showing clearly the cooling potential of PWM pattern in the parallel connected TEC system. In more details as $D_f$ decreased (narrower current pulses) and $f_s$ increased, $P_c$ became adequately high for the specific application (higher than the 7W target); it could have reached values even higher than 10W, as long as $I$ became higher than 1.5 A. On the other hand, for such high $P_c$ and small $D_f$ values, *COP* became lower than 1.0; this was due to the extremely high peak current pulses, that seriously affect the electric consumption. Moreover, as $D_f$ became higher, $P_c$ value moderated under any $f_s$ value (the operation converged towards continuous current supply operation); the *COP* factor became higher than 1.0 whereas $P_c$ decreased – although it remained at the range of 7W – for $I > 1$A. It is noted that the current-switching frequency combinations in Figs 13, 14 cover almost any possible operational condition; as it has been experimentally deduced, higher current and switching frequency values deteriorate the system operation. In conclusion, classical active PWM control is able to exploit the cooling capabilities of the parallel connected TEC system by increasing the switching frequency at the range of 10 kHz or higher. On the other hand, at higher ambient temperature values (like the one during the test) the achievement of high *COP* values, becomes more difficult due to the high current pulses that are required to keep $P_c$ high enough. A solution to this issue is the proposed active PWM control (DPC pattern), that has been developed in the context of THERMICOOL project and the experimental verification of which, will be presented next. Nevertheless, according to the obtained results in Case 4, we may conclude that the parallel TEC connection manages to operate at higher $\Delta T$ values than the ones in series connection, due to the positive effect of the high switching frequency that has been discussed. As a result, the mezzanine surface is more effectively cooled, with its average temperature being slightly higher (+3.4°C) than the target, only at very high ambient temperatures.

Last, Case 5 is the most ambitious one, because it incorporated the proposed double carrier frequency DPC pattern. As presented, a fast switching frequency (higher than 1 kHz) that determined $P_c$ and a slow switching frequency (lower than 1 kHz) that determined *COP* factor (by means of electrical consumption regulation) were used. The novel active PWM control method was tested in the parallel TEC connection, with the following technical characteristics:

- Fast switching frequency: 50 kHz
- Fast switching frequency duty cycle: 30% - 80%
- Slow switching frequency: 0,.1 Hz
- Slow switching frequency duty cycle: 70%

The obtained results highlight the effectiveness of the proposed novel active PWM control method; its application in the parallel TEC connection achieved operation at higher $\Delta T$ values than the ones with the classical (single modulation frequency) PWM control, due to the positive effect of the slow switching frequency on the electrical consumption (as already discussed). As a result, the mezzanine surface was more effectively cooled, with its average temperature meeting the target even at the highest considered ambient temperature (+95°C). It should be noted that the superior performance of DPC over SPC that is reported in this work is not a general outcome; different system configurations (including TEC material) and environmental conditions may have significant impact on the performance of the active cooling system. In addition, there is still research effort to be made in order to conclude to the optimal close loop design. Nevertheless, the introduction of the proposed novel active PWM control method in the parallel TEC connection managed to meet the project requirement; the average temperature at the mezzanine surface was kept lower than +95°C, while $P_c$ exceeded the 7W threshold.

## VI. CONCLUSION

THERMICOOL project, implemented under the CLEAN SKY framework, has proven that Thermoelectric Cooling is a viable solution for reducing the power consumption and increasing reliability of aerospace electronics. The experimental process has shown that sophisticated control loops are necessary for a successful multi-stage TEC system design under such harsh environmental conditions. In fact, TEC operation has to be active even under moderate temperature conditions, otherwise their cooling capability may be restricted in case of fast temperature rise (e.g. under the sudden raise of the consumption of the electronic equipment).

Although the outcomes for the average temperature values are generally in line with the corresponding simulation results, there are notable deviations between minimum / maximum temperature values. The main reason for this is the distribution of heat sources which was considered uniformly in the simulation model. In addition, there are some differences on the materials and the modification of the various system components between the simulation design and the experimental development. It should be noted that if a larger number of appropriately distributed thermal sources were available a closer agreement between simulations and experimental outcomes would be achieved. Nevertheless, these deviations can be justified by the research nature of the THERMICOOL project and consequently the fact that some system data were not fully determined during the simulation phase.

In conclusion, the main targets of THERMICOOL project have been successfully fulfilled, coming up with a novel active cooling method that meets the project requirements. In addition, enhanced control algorithms for multi-stage TEC schemes have been invented, calling for further research and development actions.

## ACKNOWLEDGMENT

The authors thank Mr. Christos Tsipitsoudis, member of the Technical Staff of Democritus University of Thrace, for his support on the laboratory test bench assembly as well as during the experimental evaluation procedure.

## REFERENCES

[1] J. Yang and F. R. Stabler, "Automotive applications of thermoelectric materials," in *Modules, Systems and Applications in Thermoelectrics*, D. M. Rowe, Ed. Boca Raton, FL, USA: CRC Press, 2012, ch. 25, pp. 25.1–25.15.

[2] A. D. Rosa, "Thermoelectricity," in *Fundamentals of Renewable Energy Sources*. New York, NY, USA: Elsevier, 2009, pp. 153–218.

[3] W. Brostow, G. Granowski, N. Hnatchuk, J. Sharp, and J. B. White, "Thermoelectric phenomena," *J. Mater. Edu.*, vol. 36, nos. 5–6, pp. 175–186, 2014.

[4] S. Lineykin and S. Ben-Yaakov, "Modeling and analysis of thermoelectric modules," *IEEE Trans. Ind. Appl.*, vol. 43, no. 2, pp. 505–512, Mar./Apr. 2007.

[5] C. Li, D. Jiao, J. Jia, F. Guo, and J. Wang, "Thermoelectric cooling for power electronics circuits: Modeling and active temperature control," *IEEE Trans. Ind. Appl.*, vol. 50, no. 6, pp. 3995–4005, Nov./Dec. 2014.

[6] W. Brostow and H. E. H. Lobland, *Materials: Introduction and Applications*. New York, NY, USA: Wiley, 2017, ch. 20.

[7] J.-C. Zheng, "Recent advances on thermoelectric materials," *Frontiers Phys. China*, vol. 3, no. 3, pp. 269–279, 2008.

[8] J.-F. Li, W.-S. Liu, L.-D. Zhao, and M. Zhou, "High-performance nanostructured thermoelectric materials," *NPG Asia Mater.*, vol. 2, pp. 152–158, Oct. 2010.

[9] Z. Ren, G. Chen, and M. Dresselhaus, "Nanostructured thermoelectric materials," in *Modules, Systems, and Applications in Thermoelectrics*, D. M. Rowe, Ed. Boca Raton, FL, USA: CRC Press, 2012, pp. 1–3.

[10] B. Poudel *et al.*, "High-thermoelectric performance of nanostructured bismuth antimony telluride bulk alloys," *Science*, vol. 320, pp. 634–638, Mar. 2008.

[11] C.-J. Liu, H.-C. Lai, Y.-L. Liu, and L.-R. Chen, "High thermoelectric figure-of-merit in p-type nanostructured $(Bi,Sb)_2Te_3$ fabricated viahydrothermal synthesis and evacuated-and-encapsulated sintering," *J. Mater. Chem.*, vol. 22, no. 11, pp. 4825–4831, 2012.

[12] W. Xie, X. Tang, Y. Yan, Q. Zhang, and T. M. Tritt, "Unique nanostructures and enhanced thermoelectric performance of melt-spun BiSbTe alloys," *Appl. Phys. Lett.*, vol. 94, p. 102111, Mar. 2009.

[13] W.-S. Liu *et al.*, "Thermoelectric property studies on Cu-doped n-type $CuxBi_2Te_{2.7}Se_{0.3}$ nanocomposites," *Adv. Energy Mater.*, vol. 1, no. 4, pp. 577–587, 2011.

[14] M. H. Elsheikh *et al.*, "A review on thermoelectric renewable energy: Principle parameters that affect their performance," *Renew. Sustain. Energy Rev.*, vol. 30, pp. 338–351, Feb. 2013.

[15] G. A. Slack, *Handbook of Thermoelectrics*. Boca Raton, FL, USA: CRC Press, 1995.

[16] C. Godart, A. P. Goncalves, E. B. Lopes, and B. Villeroy, "Role of structures on thermal conductivity in thermoelectric materials," in *Properties and Applications of Thermoelectric Materials*. Dordrecht, The Netherlands: Springer, 2008, pp. 19–42.

[17] J. Yang *et al.*, "Solubility study of Yb in n-type skutterudites $YbxCo_4Sb_{12}$ and their enhanced thermoelectric properties," *Phys. Rev. B, Condens. Matter*, vol. 80, no. 11, p. 115329, 2009.

[18] Q. He *et al.*, "Nanostructured thermoelectric skutterudite $Co_{1-x}Ni_xSb_3$ alloys," *J. Nanosci. Nanotechnol.*, vol. 8, no. 8, pp. 4003–4006, 2008.

[19] V. Zlatić, "Thermoelectric power of cerium and ytterbium intermetallics," *Phys. Rev. B, Condens. Matter*, vol. 68, p. 104432, Sep. 2003.

[20] T. Xinfeng, Z. Qingjie, C. Lidong, G. Takashi, and H. Toshio, "Synthesis and thermoelectric properties of p-type- and n-type-filled skutterudite $R_yM_xCo_{4-x}Sb_{12}(R : Ce, Ba, Y; M : Fe, Ni)$," *J. Appl. Phys.*, vol. 97, no. 9, p. 093712, 2005.

[21] H. Anno, H. Yamada, T. Nakabayashi, M. Hokazono, and R. Shirataki, "Gallium composition dependence of crystallographic and thermoelectric properties in polycrystalline type-I $Ba_8Ga_xSi_{46-x}$ (nominal $x = 14 - 18$) clathrates prepared by combining arc melting and spark plasma sintering methods," *J. Solid State Chem.*, vol. 193, pp. 94–104, Sep. 2012.

[22] N. Shutoh and S. Sakurada, "Thermoelectric properties of the $Ti_x(Zr_{0.5}Hf_{0.5})_{1-x}NiSn$ half-Heusler compounds," in *Proc. 22nd Int. Conf. Thermoelectrics (ICT)*, La Grande-Motte, France, 2003, pp. 312–315.
[23] D. M. Rowe, V. S. Shukla, and N. Savvides, "Phonon scattering at grain boundaries in heavily doped fine-grained silicon–germanium alloys," *Nature*, vol. 290, pp. 765–766, Apr. 1981.
[24] G. Joshi *et al.*, "Enhanced thermoelectric figure-of-merit in nanostructured p-type silicon germanium bulk alloys," *Nano Lett.*, vol. 8, no. 12, pp. 4670–4674, 2008.
[25] L.-D. Zhao, V. P. Dravid, and M. G. Kanatzidis, "The panoscopic approach to high performance thermoelectrics," *Energy Environ. Sci.*, vol. 7, no. 1, pp. 251–268, 2014.
[26] F. P. Pierre Poudeu *et al.*, "High thermoelectric figure of merit and nanostructuring in bulk p-type $Na_{1-x}Pb_mSb_yTe_{m+2}$," *Angew. Chem. Int. Ed.*, vol. 45, no. 23, pp. 3835–3839, 2006.
[27] K. F. Hsu *et al.*, "Cubic $AgPb_mSbTe_{2+m}$: Bulk thermoelectric materials with high figure of merit," *Science*, vol. 303, pp. 818–821, Feb. 2004.
[28] J. He, Y. Liu, and R. Funahashi, "Oxide thermoelectrics: The challenges, progress, and outlook," *J. Mater. Res.*, vol. 26, no. 15, pp. 1762–1772, Aug. 2011.
[29] K. Fujita, T. Mochida, and K. Nakamura, "High-temperature thermoelectric properties of $Na_xCoO_{2-\delta}$ single crystals," *Jpn. Soc. Appl. Phys.*, vol. 40, no. 7, pp. 4644–4647, 2001.
[30] M. Shikanoa and R. Funahashi, "Electrical and thermal properties of single-crystalline $(Ca_2CoO_3)_{0.7}CoO_2$ with a $Ca_3Co_4O_9$ structure," *Appl. Phys. Lett.*, vol. 82, pp. 1851–1853, Mar. 2003.
[31] R. Funahashi and M. Shikano, "$Bi_2Sr_2Co_2Oy$ whiskers with high thermoelectric figure of merit," *Appl. Phys. Lett.*, vol. 81, pp. 1459–1461, Aug. 2002.
[32] G. J. Snyder and E. S. Toberer, "Complex thermoelectric materials," *Nature Mater.*, vol. 7, pp. 105–114, Feb. 2008.
[33] D.-Y. Chung *et al.*, "$CsBi_4Te_6$: A high-performance thermoelectric material for low-temperature applications," *Science*, vol. 287, pp. 1024–1027, Feb. 2000.
[34] B. Wölfing, C. Kloc, J. Teubner, and E. Bucher, "High performance thermoelectric $Tl_9BiTe_6$ with an extremely low thermal conductivity," *Phys. Rev. Lett.*, vol. 86, pp. 4350–4353, May 2001.
[35] O. Yamashita, S. Tomiyoshi, and K. Makita, "Bismuth telluride compounds with high thermoelectric figures of merit," *J. Appl. Phys.*, vol. 93, pp. 368–374, Jan. 2003.
[36] G. C. Christidis *et al.*, "Innovative waste heat recovery systems in rotorcrafts," in *Proc. Elect. Syst. Aircraft, Railway Ship Propuls. (ESARS)*, 2012, pp. 1–4. [Online]. Available: http://10.1109/ESARS.2012.6387452

**EMMANUEL KARAMPASIS** received the Dipl.Eng. degree in mechanical engineering from the University of West Macedonia, Kozani, Greece, in 2008. He joined ITC S.A., Athens, Greece, in 2015, where he is currently a Research and Development Staff.

His research interests include the analysis, design, simulation, and construction of active thermoelectric systems for use in waste heat recovery and aeronautics applications.

Mr. Karampasis is a member of the Technical Chamber of Greece.

**NICK PAPANIKOLAOU** (M'08–SM'10) received the Dipl.Eng. and Ph.D. degrees in electrical engineering from the University of Patras, Rion-Patras, Greece, in 1998 and 2002, respectively.

He had been with the Hellenic Electric Energy Industry, for several years, where he was involved in major European transmission and generation projects. He is currently an Assistant Professor with the Department of Electrical and Computer Engineering, Democritus University of Thrace, Xanthi, Greece. His research interests include power electronics, renewable energy exploitation, distributed generation, energy saving, electric vehicles, and power quality improvement.

Dr. Papanikolaou is a member of CIGRE and the Technical Chamber of Greece.

**DIONISIS VOGLITSIS** received the Dipl.Eng. degree in electrical engineering from the Democritus University of Thrace, Xanthi, Greece, in 2008, and the M.Sc. degree in electrical engineering from the Delft University of Technology, The Netherlands, in 2014. He is currently pursuing the Ph.D. degree in grid-tied inverters for distributed generation with the Democritus University of Thrace. He joined the Electrical and Computer Engineering, Democritus University of Thrace, in 2014.

His research interests include the analysis, design, simulation, and construction of dc/dc and dc/ac converters for use in renewable energy systems, waste heat recovery systems, and aeronautics applications.

Mr. Voglitsis is a member of the Technical Chamber of Greece.

**MICHAEL LOUPIS** (M'08–SM'10) received the Dipl.Eng. degree in electrical engineering from the Aristotelian University of Thessaloniki, Greece, the M.Sc. degree in microprocessor engineering from the University of Bradford, U.K., the Ph.D. degree in electrical engineering from the National Technical University of Athens, Greece, and the M.Sc. degree in quality assurance from the Greek Open University.

He is the Technical Manager of ITC S.A., being the coordinator of various EU funded research programs and also an Assistant Professor with the Technological Educational Institute of Central Greece.

Dr. Loupis is a member of the Technical Chamber of Greece, the Association of Mechanical and Electrical Engineers, the Association of Computer Engineers, and the Greek Computer Society, a Fellow Member of the Society for Industrial Robotics and Expert Systems, and a member of the Institution of Engineering and Technology.

**ANASTASIOS PSARRAS** received the Diploma degree in electrical and computer engineering and the master's degree from the Democritus University of Thrace, Xanthi, Greece, in 2012 and 2013, respectively, where he is currently pursuing the Ph.D. degree. His current research interests include low power system-on-chip design, and particularly on on-chip interconnection networks.

**ALEXANDROS BOUBARIS** is currently pursuing the degree with the Department of Electrical and Computer Engineering, Democritus University of Thrace, Xanthi, Greece. He is currently working toward his Diploma thesis in the field of active thermoelectric cooling applications.

**DIMITRIS BAROS** received the Dipl.Eng. degree in electrical engineering from the Democritus University of Thrace, Xanthi, Greece, in 2015, where he is currently pursuing the M.Sc. degree in power electronics.

His research interests include the analysis, design, simulation, and construction of dc/dc and dc/ac converters for use in renewable energy systems, waste heat recovery systems, and aeronautics applications.

**GIORGOS DIMITRAKOPOULOS** received the B.S., M.Sc., and Ph.D. degrees in computer engineering from the University of Patras, Patras, Greece, in 2001, 2003, and 2007, respectively.

He is currently an Assistant Professor with the Department of Electrical and Computer Engineering, Democritus University of Thrace, Xanthi, Greece. He is interested in the design of digital integrated circuits and computer architecture, with emphasis in network-on-chip design and ultra-low power systems.